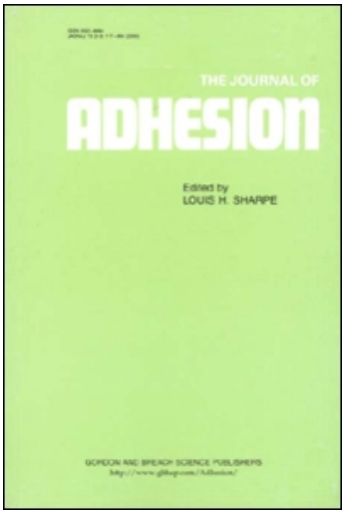

The Journal of Adhesion
Publication details, including instructions for authors and subscription information:
http://www.informaworld.com/smpp/title~content=t713453635

Aging Process of Metal/Epoxy Laminates Investigated with X-ray Photoelectron Microscopy and Spectroscopy

M. Kinzler[a]; M. Grunze[a]; N. Blank[bc]; H. Schenkel[b]; I. Scheffler[b]
[a] Angewandte Physikalische Chemie der Universität Heidelberg, Heidelberg, Germany [b] Teroson GmbH, Heidelberg, Germany [c] Sika Corporation, Lyndhurst, NJ, USA

To cite this Article Kinzler, M. , Grunze, M. , Blank, N. , Schenkel, H. and Scheffler, I.(1994) 'Aging Process of Metal/Epoxy Laminates Investigated with X-ray Photoelectron Microscopy and Spectroscopy', The Journal of Adhesion, 45: 1, 207 — 226
To link to this Article: DOI: 10.1080/00218469408026639
URL: http://dx.doi.org/10.1080/00218469408026639

J. Adhesion, 1994, Vol. 45, pp. 207–226
Reprints available directly from the publisher
Photocopying permitted by license only

Printed in the United States of America

Aging Process of Metal/Epoxy Laminates Investigated with X-ray Photoelectron Microscopy and Spectroscopy*

M. KINZLER and M. GRUNZE

Angewandte Physikalische Chemie der Universität Heidelberg, Im Neuenheimer Feld 253, 69120 Heidelberg, Germany

N. BLANK**, H. SCHENKEL and I. SCHEFFLER

Teroson GmbH, Hans-Bunte-Str. 4, 69123 Heidelberg, Germany

(Received March 9, 1993; in final form July 30, 1993)

In this article we describe the application of X-ray photoelectron spectroscopy to epoxy/dicyandiamide laminates on zinc galvanized steel which were aged under different environmental conditions involving high humidity and temperatures.

X-ray photoelectron microscopy allows us to identify the distribution of chemical elements with a lateral resolution of 10 μm. Areas selected in the microscopy mode were then analyzed in the spectroscopy mode in order to get information on the local chemical composition.

We compared the spectroscopic features of the aged but freshly delaminated surfaces of samples stored under ambient conditions at room temperature with samples exposed to the "Kataplasma" and the "KWT" test, respectively. Furthermore, a comparison was made with a model sample which was prepared in vacuum and on which the curing process was investigated.

Though there is no substantial loss in the lap-shear strength of the samples, we find drastic spectroscopic changes in the Kataplasma and KWT treated samples compared with the sample kept at room temperature. We conclude that the chemical changes induced by these tests cause an internal interphase boundary between the epoxy/metal interface and the bulk adhesive along which delamination occurs. Comparison with the behavior of the water-vapor-treated model sample gives evidence that hydrolysis is the main reaction in these tests.

The results described here complement our former study.[1]

KEY WORDS epoxy-dicyandiamide adhesive; galvanized steel; electroplated steel; adhesion; delamination; corrosion; bond strength; environmental tests; X-ray photoelectron spectroscopy.

1 INTRODUCTION

Epoxy resins are a widely used class of adhesives for metal bonding. For this reason, the investigation of these materials has been the subject of several studies

*Presented at the International Symposium on "The Interphase" at the Sixteenth Annual Meeting of The Adhesion Society, Inc., Williamsburg, Virginia, U.S.A., February 21–26, 1993.

**Current address: Sika Corporation, 201 Polito Avenue, Lyndhurst, NJ 07071, USA.

employing X-ray photoelectron spectroscopy (XPS) and infrared reflection absorption spectroscopy (IRAS). While these techniques give average information over the whole surface under investigation, we employed X-ray photoelectron microscopy (XPM) with a lateral resolution of 10 μm in order to resolve the chemical heterogeneity of the fracture surfaces.

The interfacial chemistry of an epoxy/dicyandiamide (dicy) adhesive has been studied, using XPS, by Dickie *et al.*[2] For zinc galvanized steel they find a bond failure at the adhesive/metal interface within a layer of zinc corrosion products. Infrared studies[3] suggested that at the zinc/dicy interface a reduction of the dicy occurred, resulting in a carbodiimide intermediate. Furthermore, a study by Zahir[4] showed that, upon curing, ammonia or alkylamines are eliminated from the resin.

In our previous report,[1] we found zinc ions *in the resin* after the aging process induced by the Kataplasma test and we concluded that formation of zinc/ammonia or zinc/alkylamine complexes leads to dissolution of zinc in the resin.

In this work we will discuss the spectroscopic comparison of differently-aged epoxy/dicy laminates on zinc galvanized steel. We will qualitatively discuss the influence of the water treatment on the chemistry of the epoxy resin and propose a reaction mechanism which is consistent with our spectroscopic results.

2 EXPERIMENTAL

2.1 Preparation of the Samples

The epoxy resin used in this study consisted of a mixture of diglycidylether of Bisphenol-A (DGEBA), a rubber adduct of DGEBA and a modified epoxy resin. As diluents, an aliphatic glycidylether and aromatic hydrocarbons were added, and the filler consisted of an acrylate polymer, AlMg silicate and carbon black. The curatives used were dicyandiamide (dicy) and a urea derivative.

The lap-shear samples were prepared with zinc galvanized steel coupons of 100 × 25 × 1.0 mm with an overlap of 12 mm and a bondline thickness of 0.3 mm. The steel was cold rolled steel, electroplated with 10 μm zinc (ST 14-ZE-100/100-05, DIN 17163), which was degreased twice in an ultrasonic bath in propanol prior to application of the adhesive. The bonding procedure was according to ASTM D-1002/DIN 53283: the bonds were fixed without pressure and cured in air in an oven at 180°C for 30 min.

After curing, the samples were either stored at room temperature (RT samples) or exposed to the Kataplasma (KT) test or the so-called Klimawechseltest (Temperature change test), KWT. For the KT test, the samples are coated with water saturated cotton, sealed in polyethylene bags and kept at 70°C for the selected period of time. The KWT test consists of temperature cycles from –40°C to +80°C at 80% relative humidity. All samples were exposed to these environmental tests for two weeks.

The model sample was prepared by applying some uncured resin to a zinc coated steel coupon which was previously cleaned with ethanol in an ultrasonic bath. A thin film (*ca.* 0.1 mm) was spread with a razor blade and the coated coupon was subsequently transferred into vacuum where it was cured at 180°C.

XPS measurements were performed prior to and after this curing process, *in situ*. The sample was then removed from the spectrometer and exposed to a water-saturated atmosphere at 75°C for 24 hours before it was measured again.

2.2 Lap-shear Strength Measurements

After the aging tests, the samples were delaminated by measuring the lap-shear forces in a tensile test machine at a rate of 25 mm/min. Subsequently, the samples were transferred into the photoelectron spectrometer and the delaminated surfaces were investigated by XPS.

2.3 Spectroscopic Measurements

The X-ray photoelectron spectrometer used in this study was an ESCASCOPE (Fisons Instruments). It has two modes of operation, one for standard XPS and one for X-ray photoelectron microscopy (XPM). The imaging mode with a field of view of ca. 880 × 880 μm gives information on the lateral distribution of the chemical elements in the surface. Features detected in the imaging mode are readily isolated and investigated by small spot spectroscopy with a field of view of 150 or 50 μm. This is especially helpful for the identification and the alignment of adhesively- and cohesively-failed regions in the spectrometer which are not always readily discernible in the optical image due to the inhomogeneity of the surface. The field of view is selected by means of apertures, the "large area" aperture providing the same field of view as in the imaging mode.

Image detection is with a channelplate detector where an energy-filtered image of the electrons emerging from the sample surface is formed by the electron optics. The energy/space convolution of the hemispherical analyzer is circumvented by energy filtering a Fourier transform of the image. The operation of the instrument is described in detail in Refs. 5 and 6.

To obtain the lateral distribution of a selected element, two images are taken, one at the kinetic energy of the photoelectron peak of the element and one at *ca.* 10 eV higher kinetic energy. This allows for background subtraction and for partial compensation of topographical effects in the XPS intensity.

The X-ray source is a conventional MgKα and AlKα twin anode operated at *ca.* 370 W. The experimental resolution in the spectroscopy mode for the selected pass energy (50 eV) was 0.98 eV measured on the Ag $3d_{\frac{5}{2}}$ peak of a clean silver sample. For the examination of the epoxy laminates, sample cooling was necessary in most cases to keep the pressure in the 10^{-9} mbar range.

The calibration of the binding energies is discussed in Section 3.4

3 RESULTS

3.1 Lap-shear Strengths of Epoxy/Zinc Bonds

No substantial decrease in bond strength could be detected after either the KT or the KWT test compared with the room temperature aged sample. While the RT samples exhibit a bond strength of 10.93±0.29 MPa, the KT samples have 9.13±0.27

and the KWT samples 10.25±0.55 MPa, respectively. In all cases, the mode of failure was *ca.* 80% cohesive as judged by optical inspection. In the case of cohesive failure, the bond did not break symmetrically, but there was always a "thin" and a "thick" side, *i.e.* the epoxy failed always near the zinc/metal interface (*cf.* Fig. 1). Within the thin sides, the zinc from the substrate was partially exposed.

This yielded three different areas on each of the delaminated coupons, the "thick" side with an epoxy layer of *ca.* 0.3 mm, the "thin" side with an estimated thickness of *ca.* 0.005 mm and the "adhesively" failed regions with no visible resin layer. As shown in Figure 1, we will refer to the "thick" sides as I, the "thin" sides

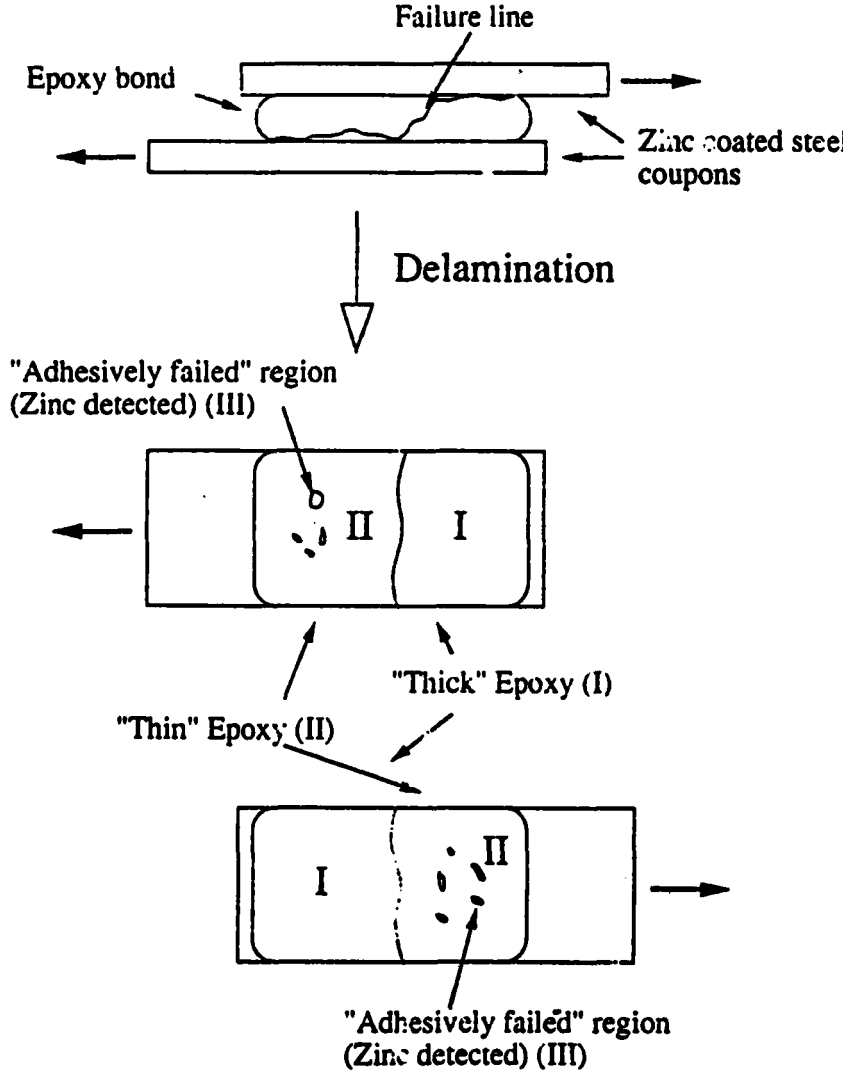

FIGURE 1 Schematic drawing of the bond failure behavior (thickness not to scale). I, II and III designate different areas which are referred to in the text.

as II, and the "adhesively" failed regions as III, irrespective of which coupon they were investigated on.

3.2 Photoelectron Microscopy

The X-ray photoelectron microscopy (XPM) mode of the ESCASCOPE allows us to distinguish clearly between adhesively- and cohesively-failed regions and to characterize the chemical heterogeneity of the fracture surfaces. In Figure 2, we show the XPM images from the KWT sample in regions II and III where metallic zinc was partly exposed after the delamination. The Zn 2p image (2a) clearly shows the "adhesively" (as judged by optical microscopy) delaminated areas, while the C 1s image (2b) shows an inverted contrast indicating a carbon depletion on the zinc areas. However, the contrast is much weaker in the C 1s image compared with the Zn 2p image and needed to be enhanced by image processing, see Figure 2b. This means that after the delamination a very thin layer of epoxy remains on the zinc which is not visible and thin enough to allow for the Zn 2p photoelectrons to escape but thick enough to give a high C 1s signal, *i.e.* the thickness is several tens to hundred Ångstroms.

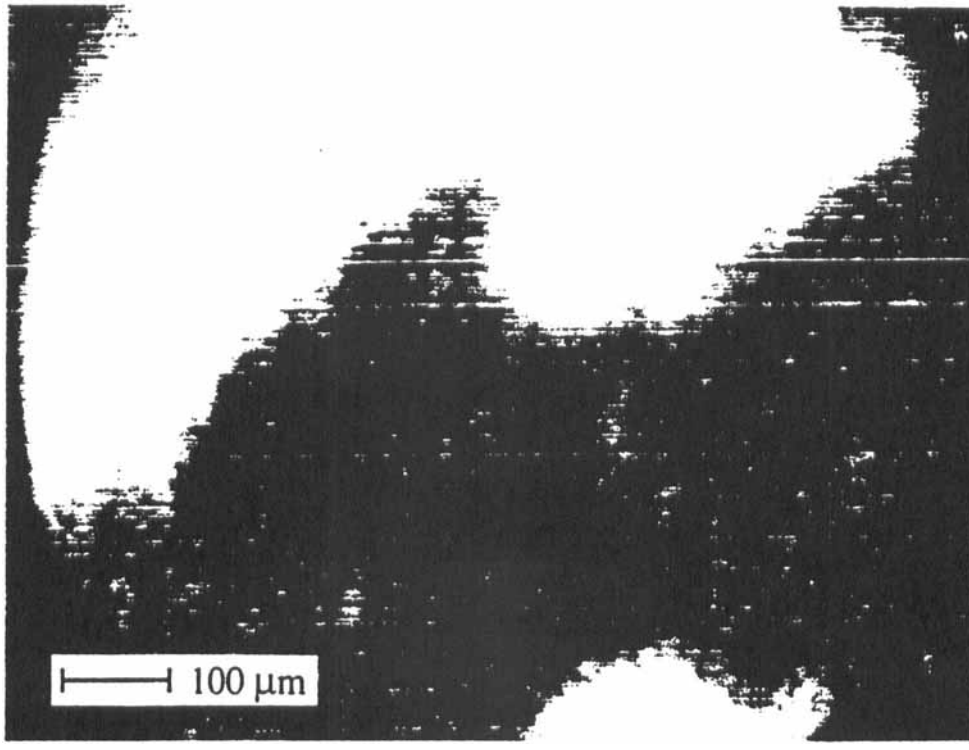

FIGURE 2 X-ray photoelectron micrograph of the KWT sample (area where II and III are visible) a: Zn 2p, b: C 1s.

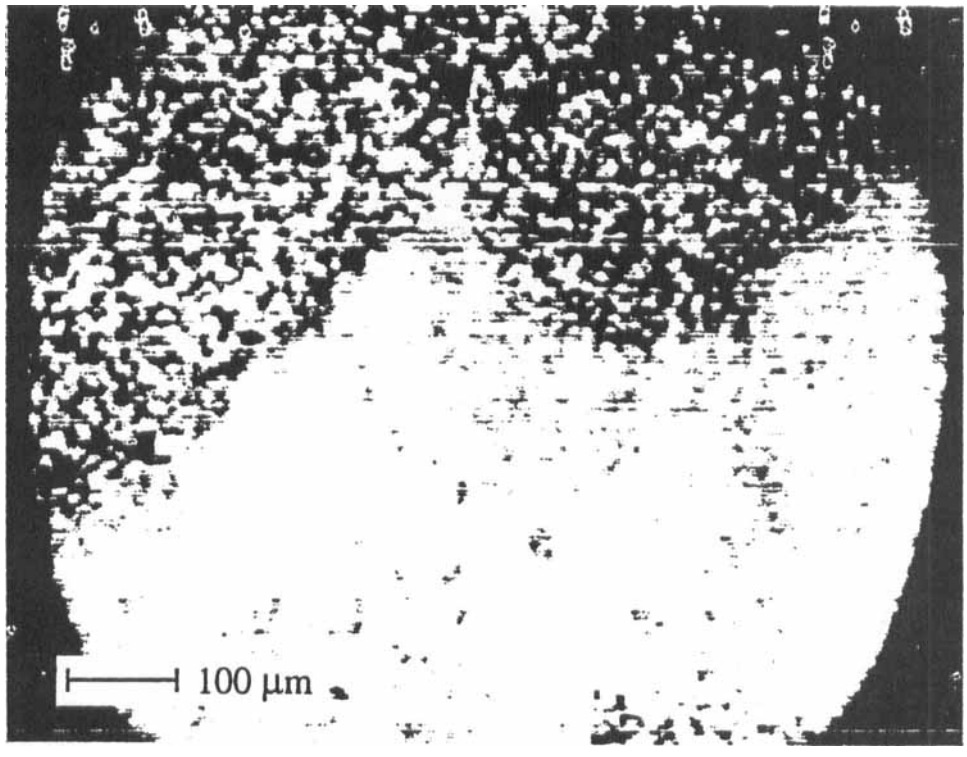

FIGURE 2 *(Continued)*

From our spectroscopic measurements (see below) we conclude that the C 1s signal from the delaminated zinc areas consists of two components, one of virtually unchanged resin and one from a polymer/metal interface layer which contributes to the total signal according to the thickness of the residual epoxy layer atop.

Another XPM result was the detection of oxygen-rich spots on different samples, *e.g.* on the thick side [I] of the KWT sample (*cf.* Fig. 3). In Figure 3a, we show the O 1s image, in Figure 3b the Si 2p image from the same area. Since the oxygen concentration coincides with the silicon distribution (see arrows), we conclude that these oxygen-rich spots represent filler particles. The O 1s contrast is weaker than the Si 2p contrast due to the epoxy oxygen which gives a high background. Note that the dark areas which are visible in both images are caused by shadowing effects due to roughness of the sample. Small spot XPS measurements of the C 1s peak did not show differences between these particles and the epoxy resin, *i.e.* again the mode of failure is cohesive rather than adhesive on the filler particle surfaces.

3.3 Photoelectron Spectroscopy

Spectroscopic measurements were carried out on the model sample (before and after heating as well as after the treatment in high humidity) and on both thin [II] and thick [I] sides of the RT, the KT and the KWT sample. On the "thin" sides,

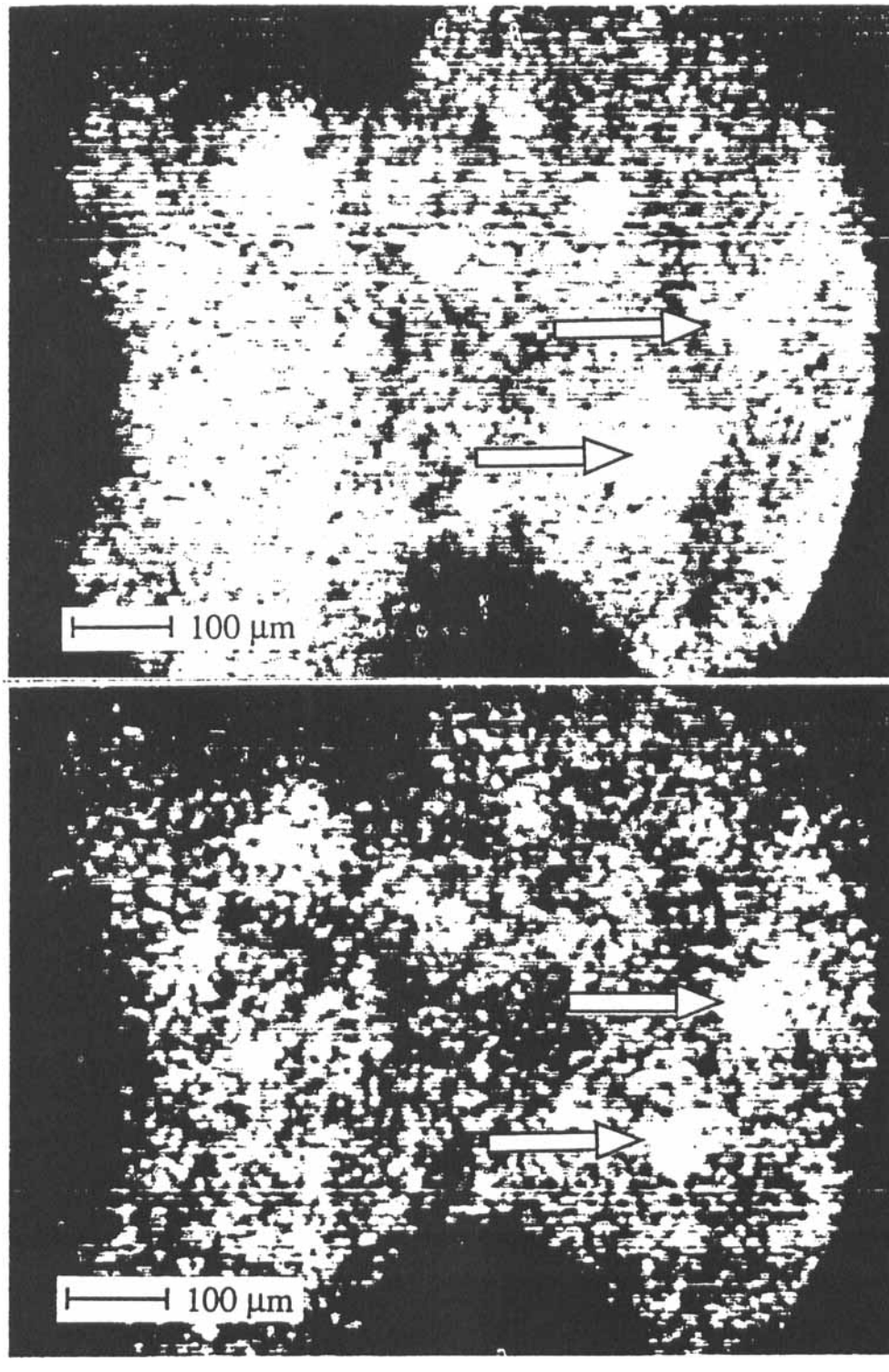

FIGURE 3 X-ray photoelectron micrograph of the KWT sample (thick side, I) a: O 1s, b: Si 2p.

areas were selected where either a visible layer of resin had remained [II] or where the zinc from the metal substrate had been exposed [III]. Spectra of the C 1s, the O 1s, the N 1s photoemission peaks and, on the [III] sides, the Zn 3p features, were recorded with a pass energy of 50 eV. All spectra shown here were recorded using MgKα radiation.

The spectra were deconvoluted using our own software in order to determine binding energies and full widths at half maximum (FWHM's). The software allows subtraction of a Shirley background and peak fitting with Gaussian lineshapes. The spectra displayed in Figures 4 to 10 were calibrated against the main component of the C 1s emission which was set to 284.6 eV, the value for aliphatic hydrocarbons which are the main component of the epoxy under investigation. This procedure differs from that applied in our previous report (see below).

In Figure 4, we compare the C 1s emission of the uncured resin (a) with the emission of the vacuum-cured resin (b), the humidity-treated resin (c), the RT sample (d), the KT sample (e) and the KWT sample (f). Figure 5 displays the fits for the cured resin (a), the RT sample (b) and the KT sample (c). All spectra were taken from areas covered with a thick layer of epoxy [I]. Numbers in italics designate the components obtained by fitting the data. These numbers are referred to in the text and in the tables.

As can readily be seen, the emission from the uncured resin (4a) is split into two components at 284.6 eV (FWHM 1.4 eV) and 286.3 eV (FWHM 1.5 eV). After curing (4b/5a), the component at 286.3 eV (2) is almost as strong as the lower binding energy feature (*1*). There is an additional feature at 288.1 eV (FWHM 2.0 eV, *3*) which we ascribe to carbonyl groups in the cured resin, probably from the acrylate filler. Upon humidity treatment (4c), component *2* becomes weaker and the peaks are broadened to *ca.* 1.7 eV so that the components are no longer resolved in the spectrum. A weak carbonyl feature (*3*) can be fitted into the spectrum at 288.0 eV, FWHM 2.3 eV.

In the RT sample (4d/5b), the peak widths for components *1* and *2* have broadened to 2.0 eV and 1.5 eV, respectively. The carbonyl emission (*3*) is found at 287.8 eV with a FWHM of 2.9 eV.

In the KT [I] (4e/5c) and the KWT [I] (4f) spectra, a further peak broadening of the high binding energy feature near 286.2 eV to 2.3 eV is observed, whereas the FWHM of the hydrocarbon component (*2*) remains at *ca.* 1.9 eV. No carbonyl emission is detected in these humidity-treated samples.

By carefully aligning the samples in the spectrometer, we tried to find spectroscopic differences between the [I] surfaces formed by "cohesive" delamination and [I] areas formed complementary to "adhesively" failed [III] regions, *i.e.* regions on the thick epoxy sides [I] that exposed epoxy broken near the metal/polymer interface.

No significant spectroscopic differences and virtually no zinc could be found on the epoxy [I] opposite to the "adhesively" failed areas [III], *i.e.* the locus of failure must be inside the epoxy. Only for the case of the KT sample, minor amounts of zinc could be detected as described in Ref. 1; X-ray photoelectron microscopy (not shown) revealed that the zinc was homogeneously distributed in the polymer matrix. Thus we can exclude the transfer of zinc particles from the substrate which could arise from the plate-like morphology of the electroplated zinc. Note,

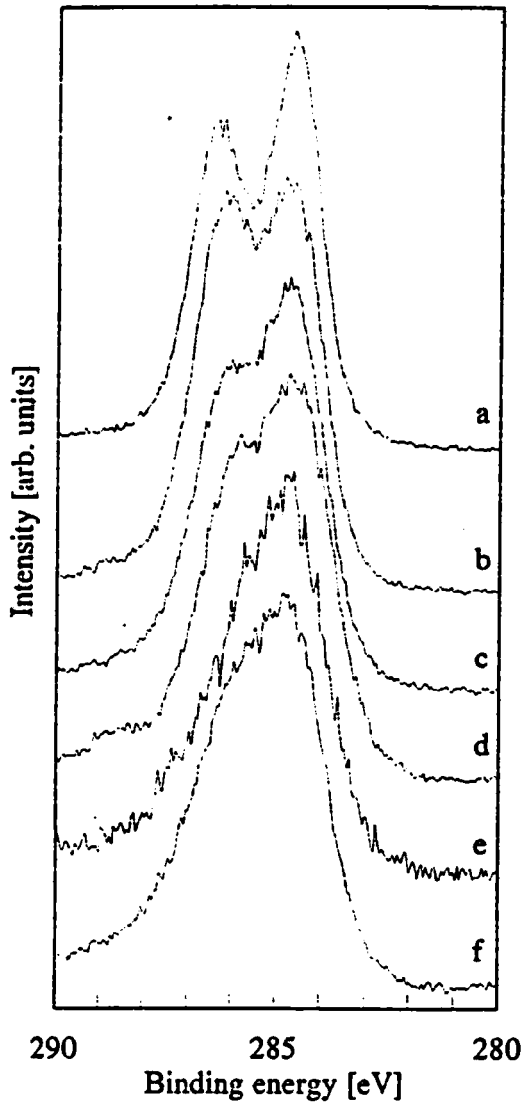

FIGURE 4 C 1s spectra of thick epoxy a: model epoxy uncured, b: model epoxy after heating, c: model epoxy after water treatment, d: RT [I], e: KT [I], f: KWT [I] treated coupons.

however, that we find differences in the C 1s spectra of the thick epoxy sides [I] and the thin sides [II] (described below).

In the O 1s spectra of the [I] samples (not shown here), we find a peak which can be fitted with a single Gaussian (component *1*). In the model sample, after heating, it is at *ca.* 532.5 eV, FWHM 1.8 eV (1.6 eV before heating). While the binding energy remains constant in all samples, it broadens substantially with the aging process (FWHM is 2.5 eV in the KT sample).

For the N 1s spectra (also not shown), the picture is the same: the peak energy

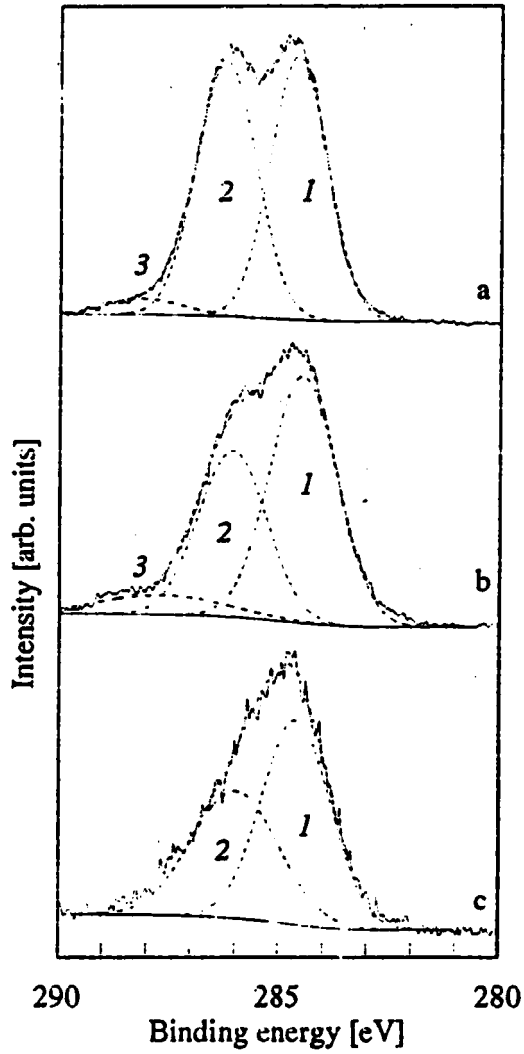

FIGURE 5 Deconvolution of C 1s spectra: a: Model epoxy after heating, b: RT [I] sample, c: KT [I] sample.

is always near 399.5 eV, the FWHM increases from 2.0 eV in the cured sample to 2.8 eV in the KWT sample (component *1*). Since the signal/noise ratio is rather bad in these spectra, the fit to the data is not very reliable.

3.4 Calibration of the Binding Energies on the [III] Sides

As mentioned above, all spectra displayed here were calibrated setting the main component of the C 1s emission (*1*) to 284.6 eV. On the polymer [I and II] sides of the samples this calibration gave reasonable results, whereas on the zinc areas [III], shown in Figures 6 to 8 this calibration is not meaningful as described below.

Figure 6 shows the C 1s spectra plotted against their corrected binding energies from the delaminated zinc surfaces where no visible resin layer had remained, *i.e.* the "adhesively-failed" regions [III] from the RT sample (a), the KT sample (b) and the KWT sample (c).

Since the samples in this study are insulating, it is clear that, in order to facilitate comparison between different samples, a charging shift correction has to be applied. The standard reference used in the literature,[2] and in this work for type [I] and [II] surfaces, is to set the main peak from the epoxy (*1*) to the value of aliphatic hydrocarbons (284.6 eV). Trying to do this on type [III] surfaces, however, we were confronted with one severe problem, *i.e.* the low binding energy

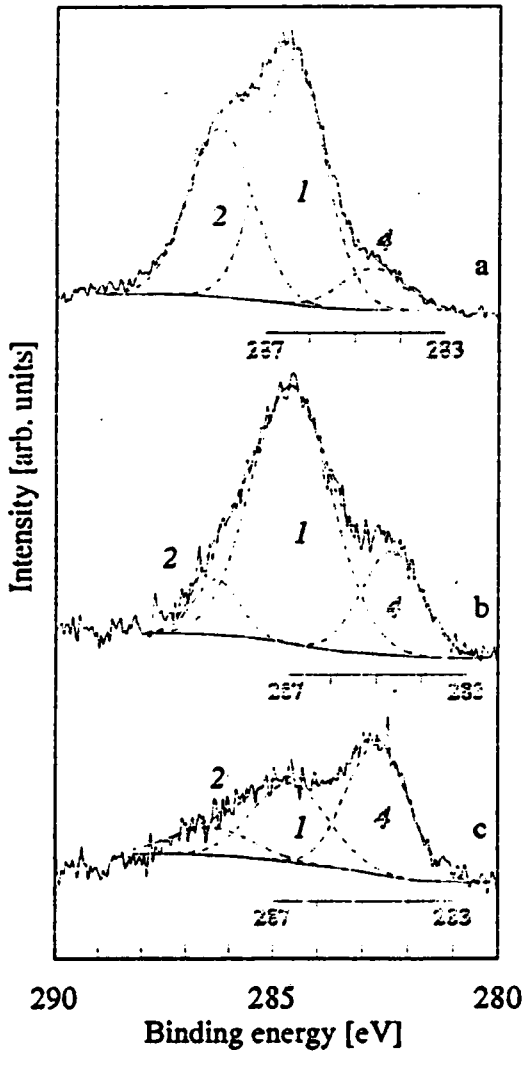

FIGURE 6 C 1s spectra from delaminated zinc surfaces [III] a: RT, b: KT, c: KWT. Individual binding energy scales are given for component *4*.

emission (*4*) was shifted to binding energies lower than tabulated values for any known compound. In our first study,[1] we thus decided to use the emission from the cured model sample at 286.1 eV as a reference to avoid this problem.

After close inspection of the data, it became clear that these "shifts" could be explained by considering a differential charging of a thin epoxy overlayer on the exposed zinc surface. Note that this problem only occurred on the [III] sides whereas, on the other samples, the binding energy reference 284.6 eV gave satisfactory results.

The sample surface of type [III] is made up of three layers, which are detected simultaneously by XPS. The charging shift of the substrate, which obviously consists of zinc oxide, can be determined using the low binding energy component (*3*) of the O 1s peak in the [III] areas which is attributed to zinc oxide (*cf.* Fig. 7). The

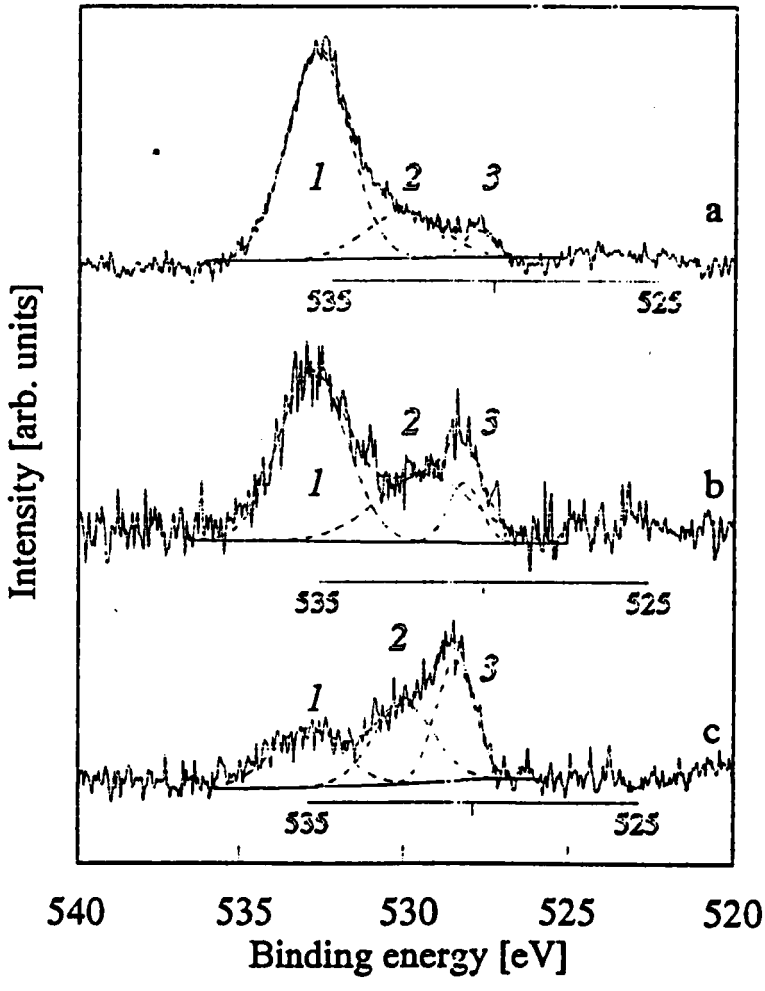

FIGURE 7 O 1s spectra from delaminated zinc surfaces [III] a: RT, b: KT, c: KWT. Individual binding energy scales are given for components *2* and *3*.

literature value for the O 1s binding energy of ZnO is 530.5 eV.[7] By comparison with the measured values (see Table I), the charging shift can be calculated. For the case of the RT III and the KWT III samples, it is 531.2—530.5=0.7 eV, whereas for the KT III sample, we find 0.6 eV.

Accordingly, the O 1s components which are ascribed to hydroxide moieties (*2*) are corrected to 532.8, 531.7 and 532.1 eV for the RT, KT and KWT samples, respectively. Note that the binding energy assignment is not quite reliable because of the low intensity.

If we employ these corrections to the [III] samples, the C 1s and O 1s emission of the *epoxy* residues (components *1* and *2* for C 1s and *1* for O 1s) are observed at far too high binding energies. This can be explained by differential charging of the epoxy residues with respect to the zinc oxide.

If the low binding energy components (*4*) in the C 1s spectra were coming from chemical species in electrical contact with the zinc oxide surface layer, they should have the same binding energies on all samples after charge correction of the zinc oxide O 1s emission. We find, however, that on the RT III sample, this C 1s component (*4*) is corrected to 285.5 eV, whereas on the KT and KWT III surfaces, a binding energy of 284.7 eV is obtained. This can be explained by an additional interface layer which is shifted with respect to the O 1s peak of zinc oxide by 0.9 eV (RT) and 0.1 eV (KT, KWT), respectively, assuming that the correct binding energy of the carbonaceous residue (possibly contaminants) is 284.6 eV. It is noteworthy that we can assume the O 1s (*2*) signal to come from this interface layer as well. This results in corrected binding energies of 531.9, 531.6 and 532.0 eV for the RT III, KT III and KWT III samples, respectively, *i.e.* the values are more consistent. This may indicate that the signal comes from the interface layer rather than from the substrate.

The remaining components which are ascribed to epoxy (because of their peak shape which closely resembles that of the bulk epoxy) are even more positively charged with respect to the zinc oxide surface. If we take as a reference the main hydrocarbon peak (*1*) with a binding energy of 284.6 eV, the differential charging

TABLE I
Measured peak positions from epoxy laminates

Sample	C 1s				O 1s			N 1s	
Component	*1*	*2*	*3*	*4*	*1*	*2*	*3*	*1*	*2*
Mod. uncured	286.0	287.7	—	—	534.2	—	—	401.0	—
Mod. heated	286.1	287.8	289.6	—	534.0	—	—	401.4	—
Mod. water	287.9	289.5	291.3	—	535.9	—	—	403.0	—
RT I	288.3	290.0	291.5	—	536.3	—	—	403.0	—
RT II	288.8	290.5	292.9	—	536.8	—	—	403.6	—
RT III	288.0	289.7	—	286.2	536.1	533.5	531.2	402.6	400.2
KT I	288.1	289.5	—	—	536.2	—	—	404.0	—
KT II	287.6	289.0	—	—	535.6	—	—	402.4	—
KT III	287.6	289.3	—	285.3	535.7	532.3	531.1	—	—
KWT I	298.6	291.2	—	—	537.6	—	—	404.6	—
KWT II	288.7	290.1	—	—	536.6	—	—	403.5	—
KWT III	287.4	289.2	—	285.4	535.7	532.8	531.2	—	399.8

is 2.7, 2.4 and 2.1 eV for the RT, KT and KWT [III] samples, respectively.

Hence, we show the spectra from the type [III] regions in Figures 6 to 8 with two binding energy scales which correspond to the two charging corrections described above. The common scale is valid for the correction of the C 1s epoxy peak (*1*) to 284.6 eV, *i.e.* for the residual epoxy layer, whereas the individual scales give the binding energy values corrected for the differential charging. In Table II, the corrected binding energies are displayed.

The RT [III] sample (Fig. 6a) shows a C 1s spectrum quite similar to that of the corresponding epoxy side with respect to the intensity ratio of the main components (*1* and *2*). There is an additional low binding energy feature (*4*) at 284.6 eV (FWHM 1.7 eV) from the interfacial layer which, according to our discussion above, is separated from the epoxy peak due to the differential charging. The intensity of this low binding energy feature (*4*) is increased after the KT test (b) and becomes the dominant peak after the KWT test (c).

Accordingly, the O 1s spectra (Fig. 7) show zinc oxide features, (*3*), at 530.5 eV and hydroxide peaks (*2*) at 532.8 eV (RT, Fig. 7a), 531.7 and 532.1 eV (KT (b), KWT(c)), respectively, besides the original O 1s peak from the epoxy (*1, ca.* 532.7 eV). Again, the contribution from the substrate/epoxy interface is strongest after the KWT test. Note that the individual binding energy scales give the correct values for oxide and hydroxide features on the ZnO surface (components *2* and *3*). Assumption of component *2* as originating from the interface layer would result in a third set of binding energy scales.

The N 1s spectra from the adhesively-failed regions are shown in Figure 8. The binding energies stated below are calculated assuming the shifted emission to come from the substrate layer. In the RT sample (a), an additional low binding energy feature (*2*) is detected at 399.5 eV on the zinc besides the original N 1s

TABLE II

Peak positions from epoxy laminates after charge correction for the C 1s main component set to E_B=284.6 eV and additional correction for differential charging on [III] samples (see text). Numbers in italics refer to the binding energy values assumed in the calibration process. The O 1s and N 1s (*1*) peaks are corrected for the C 1s epoxy peak at 284.6 eV. The O 1s and N 1s (*2*) peaks are corrected for ZnO charging by setting the oxide O 1s emission (*3*) to 530.5 eV

Sample	C 1s				O 1s			N 1s	
Component	*1*	*2*	*3*	*4*	*1*	*2*	*3*	*1*	*2*
Mod. uncured	*284.6*	286.3	—	—	532.8	—	—	399.6	—
Mod. heated	*284.6*	286.3	288.1	—	532.5	—	—	399.9	—
Mod. water	*284.6*	286.2	288.0	—	532.6	—	—	399.7	—
RT I	*284.6*	286.3	287.8	—	532.5	—	—	399.3	—
RT II	*284.6*	286.3	288.7	—	532.6	—	—	399.4	—
RT III	*284.6*	286.3	—	*284.6*	532.7	532.8	*530.5*	399.2	399.5
KT I	*284.6*	286.0	—	—	532.7	—	—	400.5	—
KT II	*284.6*	286.0	—	—	532.6	—	—	399.4	—
KT III	*284.6*	286.3	—	*284.6*	532.7	531.7	*530.5*	—	—
KWT I	*284.6*	286.2	—	—	532.6	—	—	399.6	—
KWT II	*284.6*	286.0	—	—	532.5	—	—	399.4	—
KWT III	*284.6*	286.4	—	*284.6*	532.9	532.1	*530.5*	—	399.1

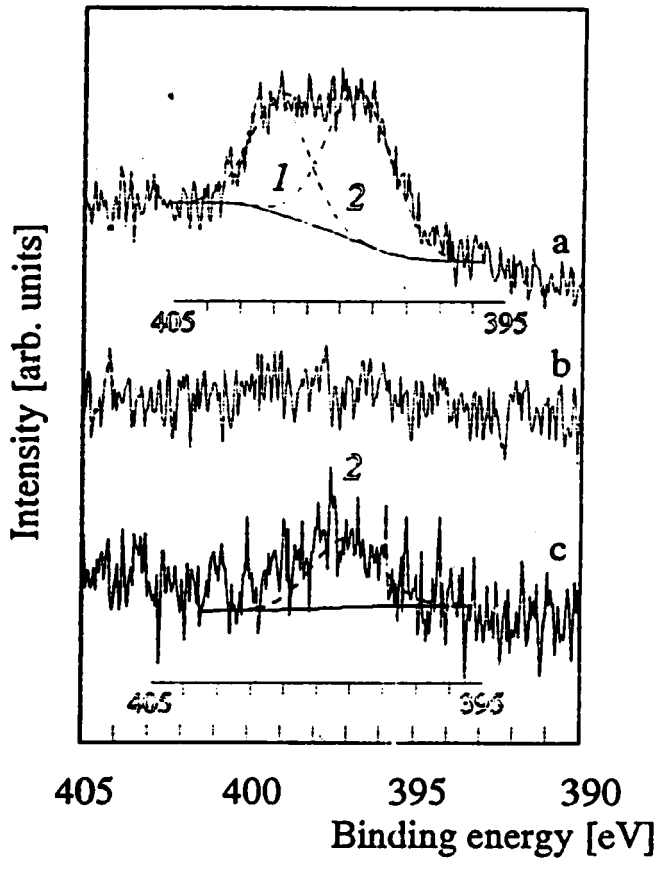

FIGURE 8 N 1s spectra from delaminated zinc surfaces [III] a: RT, b: KT, c: KWT. Individual binding energy scales are given for component *2*.

peak from the epoxy at 399.2 eV (*1*). As for the O 1s spectra, we can assume the nitrogen (*2*) component as coming from the interface, yielding binding energies of 398.6 and 399.0 eV, respectively. The KWT treated sample (c) exhibits only one peak from the interface (*2*) at 399.1 eV. The KT sample (b) shows only a very weak and broad emission in the energy range of the N 1s peak.

4 DISCUSSION

Since the epoxy resin under investigation is a commercial product containing several additives, the spectra are impossible to interpret in terms of specific chemical compounds. Some uncertainty about the true binding energies of the species observed in the spectra is caused by the rather complicated charging shifts caused by the heterogenous nature of the samples. We, therefore, discuss our results only in terms of the relative changes in the concentration of the functional groups involved in the aging process.

4.1 Epoxy Surfaces [I and II]

Most interesting is the behavior of the peaks contained in the C 1s envelope. The main components are assigned to hydrocarbons (*1*) and to carbon singly bonded to highly electronegative elements, i.e. oxygen and nitrogen (*2*). The value for the higher binding energy component (286.4 eV) is in good agreement with the tabulated values for C—O single bonds.[8] The carbonyl emission (*3*) is corrected to 288.0 eV after our calibration procedure, *i.e.* the literature value of acetone.

Most prominent in the epoxy C 1s spectra is the change in the intensity ratio between the two main components, *i.e.* the gradual loss of the high binding energy feature (*2*). Dickie *et al.*[2] find a similar behavior in their study for the epoxy side of adhesively-failed zinc/epoxy interfaces. However, since they also find signficant amounts of zinc in these surfaces, they ascribe these spectral changes to a layer of carbonaceous contaminants from the substrate which was transferred to the adhesive during the delamination and is thus being detected by the spectrometer.

In our study, we can detect a very weak zinc peak in the [I] and [II] samples only after the KT test,[1] revealing that the spectral change in the C 1s emission is really a feature of the epoxy itself and not due to contaminants. Since the main reaction between epoxy and dicy, the ring opening of the DGEBA with formation of α-hydroxyalkylamines, should not alter the spectra to such an extent, the change must be due to loss of C—O and C—N bonds during the aging process. This could be facilitated by hydrolysis of the ether bonds in the DGEBA. The small polar organic molecules thus formed could then be washed away (KT test) or segregate into the bulk epoxy or to the zinc surface. This assumption is supported by the comparison of the thin and the thick epoxy sides of cohesively-failed regions.

In Figure 9, we compare the C 1s data for the thick (I, a) and the thin (II, b) epoxy side of the KT sample. The high binding energy shoulder is weaker on the thin side. Furthermore, the peaks are broadened substantially on the thin side compared with the thick side (*cf.* Fig. 10 which shows the fits for the thick (a) and thin (b) side). The FWHM's are 2.1 and 3.0 eV [II] compared with 1.8 and 2.3 eV [I], respectively.

The same is true for the KWT sample (Fig. 9c and d). The intensity ratio between the two main components (*1* and *2*), which is 1.0 for the cured model, grows to *ca.* 1.2 to 1.4 for the water-vapor-treated model and the thick sides [I] of all samples. For the thin sides [II] of the KT and the KWT sample, the ratios are 3.1 and 2.1, respectively. As we do not detect such differences in the RT sample (Fig. 9e and f, the ratio is 1.4 for both sides of the sample), we conclude that this must be due to the humidity treatment during the aging tests. As the ratio is largest for the thin side of the KT sample, it seems that for the bulk epoxy (but not for the polymer/metal interface, see above), the KT test induces the strongest chemical changes. The C 1s spectra of the two opposite sides are different, which reveals that bond fracture occurs along an internal chemical phase boundary. This is possibly reflected also by the slight decrease in bond strength for the KT sample as found in the lap-shear strength measurements.

The oxygen (*1*) on the epoxy surfaces [I] and [II] is found at *ca.* 532.7 eV which corresponds to ether oxygen, the N 1s peak (*1*) from the epoxy is corrected to *ca.* 399.6 eV which is slightly above the value for aliphatic amines (corrections for C 1s (*1*) at 284.6 eV).

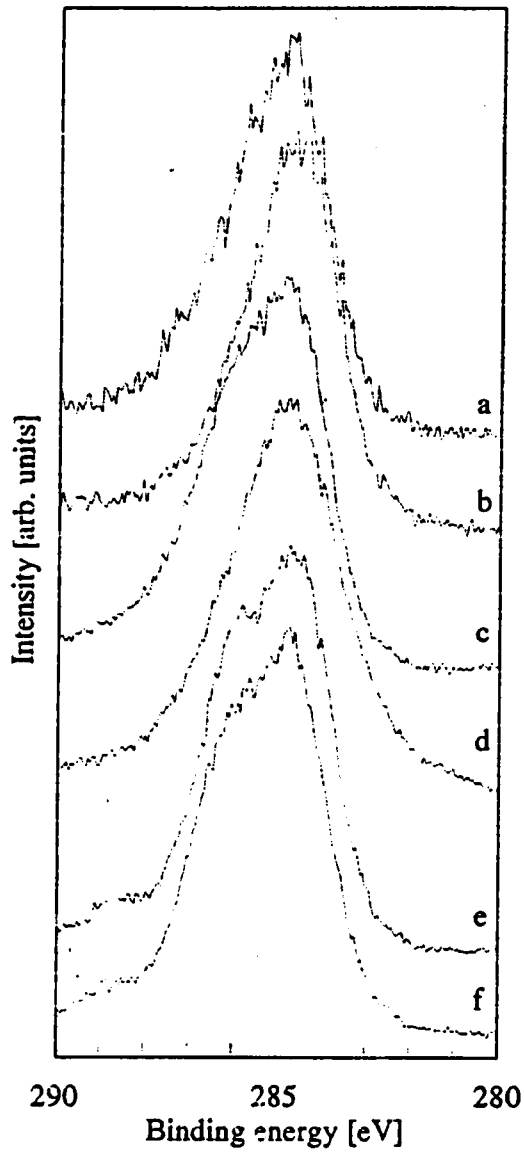

FIGURE 9 C 1s spectra: a: KT thick [I], b: KT thin [II], c: KWT thick [I], d: KWT thin [II], e: RT thick [I], f: RT thin [II].

The peak broadening in the O 1s spectra (not shown) does not give specific information about the chemical composition in the samples, but we conclude that new oxygen-containing species with slightly different binding energies are formed during the humidity treatment in support of the reaction path discussed above. It it noteworthy that the oxygen peak shows a broadening of more than 15% on the thin sides compared with the thick sides of the KT and KWT samples, but not the

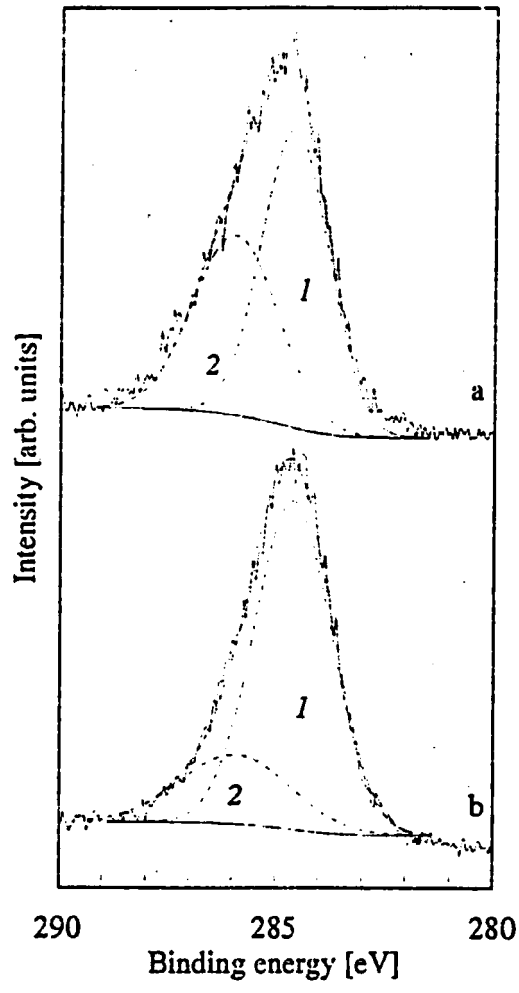

FIGURE 10 Deconvolution of C 1s spectra: a: KT thick side [I], b: KT thin side [II].

RT sample. This is the same behavior as for the C 1s spectra and indicates that this change is due to the humidity treatment leading to water absorption in the polymer. Note that the hydrocarbon component in the C 1s spectra is less affected than the higher binding energy component (at least on the thick [I] epoxy sides), so that a peak broadening due to inhomogenous charging effects can be excluded. This result also supports our conclusion that bond failure occurs along a chemical phase boundary located in the interphase between substrate and polymer.

4.2 Zinc Surfaces [III]

On the zinc surfaces [III], we find a C 1s emission from the interface layer besides the peak from the epoxy (*4*). We can not distinguish whether this emission comes from epoxy in this interface layer or from contaminant carbon which was present

prior to the bond formation. Although the component from the interface is strongest after the KWT test, the contribution from the epoxy is always observed. This indicates that the bond failure happens within the epoxy and not between the contaminant carbon and the epoxy.

The value for the hydroxide peaks (*2*) corrected for the O 1s binding energy of ZnO is around 532.0 eV for all samples, which is in agreement with the literature value for zinc hydroxide.[7]

As for the C 1s spectra, the spectral changes on the [III] regions are strongest after the KWT test, *i.e.* the interface-related emission is strongest after this test. The leads to the conclusion that either oxide and contaminant formation is more pronounced in the case of the KWT sample, or that the residual epoxy layer is thinner in this case. A possible explanation for this behavior is that the temperature changes associated with the KWT test can lead to mechanical stress and microcrack formation in the sample. Water could then easily diffuse into the polymer along micro-cracks due to the capillary forces.

The low binding energy feature in the N 1s spectra (*2*) corrected to the ZnO feature is at 399.5 eV (RT) and 399.1 eV (KWT). This is fairly compatible with tabulated binding energies for amines and cyanides.[8]

Most interesting in the N 1s spectra is the low binding energy feature on the adhesively-failed zinc surfaces (Fig. 8). The RT sample exhibits this peak along with an unchanged epoxy peak, while the KWT sample only shows the low binding energy feature (a small unchanged component may be hidden in the noise of this spectrum relates to the C 1s spectra where we find residual epoxy). Because the low binding energy feature is so much more pronounced after the KWT test as compared with the RT or KT samples, this indicates that the formation of this peak is caused by the aging process, *i.e.* humidity rather than by reaction with the zinc or zinc oxide surface alone, *i.e.* water again seems to play an important role. As the formation of amines is a possible reaction as described in Ref. 9, a formation of zinc/amine complexes can be assumed. The low binding energy of this feature is also compatible with the presence of cyano nitrogen. Cyanides and also dicy itself can form complexes with zinc, so that this is another possible reaction.

The complete loss of nitrogen at the failure line of the KT sample can then be explained by dissolution and washing away of the soluble zinc complexes by water during the KT test.

5 CONCLUSIONS

Since the spectroscopic differences in the C 1s peak between the thin and the thick side are reproducible, and representative over the surfaces of all samples studied for both aging tests, and since they result in the same change in the water-vapor-treated model sample as compared with the cured model, we conclude that "cohesive" bond failure occurs at or near an interphase boundary inside the epoxy. It seems that this boundary moves from the epoxy/zinc interface towards the bulk epoxy during the aging tests and that the locus of failure accordingly propagates in the interphase region. This is supported by the observation that the failure always occurs near the epoxy/metal interface and never in the "bulk"

epoxy. An interphase boundary is also found in a recent infrared study by Gaillard *et al.*[10] Note that the lap-shear strength is only slightly reduced by this boundary, at least under the test conditions applied. Prolonged exposure to corrosive conditions may change the mode of bond failure resulting in the well-known anodic dissolution failure.

Hydrolysis seems to be the main reaction, by which small polar molecules are formed that can react with the zinc or zinc oxide surface. Thus, water soluble complexes are formed which, in turn, can diffuse into the epoxy matrix (in the case of the KT test). The "adhesive" failure detected by optical inspection is not truly adhesive, since we always detect a thin layer of epoxy on the metal. Furthermore, small spot XPS reveals that the filler particles identified by XPM are also covered with epoxy, thus revealing the "cohesive" mode of the bond failure at the particle surfaces.

Acknowledgement

We thank Dr. C. R. Brundle for valuable discussions. Partial support for this project was received from the Deutsche Forschungsgemeinschaft (Az Gr 625/13-1).

References

1. M. Kinzler, M. Grunze, N. Blank, H. Schenkel and I. Scheffler, *J. Vac. Sci. Technol. A* **10**(4), 2691 (1992).
2. R. A. Dickie, J. W. Holubka and J. E. Devries, *J. Adhesion Sci. Technol.* **4,** 57 (1990).
3. R. O. Carter III, R. A. Dickie and J. W. Holubka, *Ind. Eng. Chem. Res.* **28,** 48 (1989).
4. S. A. Zahir, *Adv. Org. Coat. Sci. Technol. Ser.* **4,** 83 (1982).
5. P. Coxon, J. Krizek, M. Humpherson and I. R. M. Wardell, *J. Electron Spectrosc. Relat. Phenom.* **52,** 821 (1990).
6. E. Adem, R. Champaneria and P. Coxon, *Vacuum* **41,** 1699 (1990).
7. G. Deroubaix and P. Marcus, Surf. Interf. Anal. **18,** 39 (1992).
8. *Handbook of x-ray photoelectron spectroscopy*, G. E. Muilenberg, Ed. (Perkin Elmer Corp., Eden Prairie, MN, 1979).
9. M. D. Gilbert and N. S. Schneider, *Macromolecules* **24,** 360 (1991).
10. F. Gaillard, D. Verchère, H. Hocquaux and M. Romand. *J. Adhesion,* submitted for publication.